AUT Journal of Civil Engineering

AUT J. Civil Eng., 5(4) (2021) 543-556
DOI: 10.22060/ajce.2022.18056.5657

Free Vibration of Axially Functionally Graded Tapered Micro-Beams Considering Uncertain Properties

F. Kamali, F. Shahabian

Civil Engineering Department, Ferdowsi University of Mashhad, Mashhad, Iran.

ABSTRACT: Experimental observations reveal that the classical continuum theory cannot accurately describe the mechanical behavior of micro/nanoscale structures. In fact, the size-effect will arise when the order of structure dimensions is the same as the material characteristic length. The current work presents free vibration and stability of axially functionally graded (AFG) tapered micro-beams with random properties. The size-dependent behavior of the micro-structure is modeled by the modified couple stress theory. The mathematical formulations are developed based on the Euler-Bernoulli beam model and von Kármán geometric nonlinearity. The minimum total potential energy principle is employed to obtain governing differential equations and the corresponding boundary conditions. The governing equations are solved by the Galerkin method. Due to the complexity of the fabrication process of FGMs, their mechanical and structural properties may vary from sample to sample significantly. Hence, achieving the desired FGMs specification is almost impossible and they are not deterministic, inherently. To incorporate uncertainties in the mathematical model of this study, a First-Order Second-Moment (FOSM) technique is applied to estimate the reliability index of the micro-structure, stochastically. Finally, numerical examples are presented for both deterministic and reliability analysis to show the effects of geometry, length scale parameter, material distribution, and axial load on the natural frequency of vibration and the reliability index of the AFG tapered micro-beam. It can be concluded that by increasing the coefficient of variation (COV) of random variables, the reliability index will decrease. Indeed, by enhancing the length scale parameter, a higher natural frequency of vibration is expected.

Review History:

Received: Mar. 07, 2020
Revised: Jul. 03, 2021
Accepted: Jan. 25, 2022
Available Online: Feb. 03, 2022

Keywords:

Axially functionally graded
Micro-beam
Size-dependent behavior
Modified couple stress theory
First-Order Second-Moment technique
Reliability index

1- Introduction

Recently, micro/nanoscale elements have been commonly used in different high-tech instruments such as micro-actuators [1], micro-sensors [2], atomic force microscopes [3], and fuel cells [4]. Realizing the mechanical behavior of these valuable devices is essential for precise analysis and optimal design. Sometimes, elements in these instruments are utilized in which their structural behavior is like a beam. For this reason, scholars are interested to study the mechanical characteristics of the micro/nanobeam structures.

Contrary to macro scales, experimental observations show the mechanical (as well as physical and chemical) properties of materials vary with the dimensions of the structure in micro scales [5, 6]. Unfortunately, classical continuum theory cannot model the size-dependent mechanical behavior of micro/nanoscale structures, accurately. However, in recent years, researchers developed non-classical continuum theories such as Eringen's nonlocal [7] and strain gradient elasticity [8] to capture the size effect. In this respect, one of the well-known higher-order continuum theories is the couple stress. First, it was proposed by the Cosserat brothers [9] and modified many times by other scholars [10-12].

A new class of composites called functionally graded materials (FGMs) has emerged, recently. Material properties such as Young's modulus, Poisson ratio, and density in FGMs may vary continuously in a specific direction of a continuum. It should be noted that the fabrication of FGMs is a very intricate process. For this reason, achieving to desired material distribution gradient is almost impossible. FGM properties may differ from sample to sample [13]. Hence, its properties can be treated as random variables. In other words, deviation relating to the manufacturing process should be considered. Due to FGMs fabrication uncertainties, stochastic modeling of these structures may lead to a more safe and reliable design.

Several methods have been employed by researchers for stochastic modeling of FGM structures [14-16]. Among them, Monte Carlo Simulation (MCS) and First-Order Second-Moment (FOSM) techniques are the most common [17]. It should be mentioned that the MCS method is the most accurate. The advantage is that the probability distributions of random parameters can be easily found in stochastic modeling of the structure. There is no difficulty in the

*Corresponding author's email: shahabf@um.ac.ir

modeling of correlations and related variables. On the other side, MCS may be extremely time-consuming when a large number of simulations is required. However, FOSM uses the first-order derivative of a limit state function concerning the random variables in Taylor series expansion, and the higher-order terms are neglected. Indeed, the variations of random parameters are considered to be small in comparison with corresponding mean values. It should be noted that small variability is needed in parameters. Moreover, the FOSM cannot model probability distributions of uncertain variables.

Now, a brief literature review of related research will be presented, here. Wang et al. [18] investigated a Timoshenko micro-beam model using strain gradient theory. To capture the size effect, the model includes three material length scale parameters. Free vibration and static bending behavior of a hinged-hinged micro-beam are solved. Applying the consistent couple stress theory, Patel et al. [19] presented a simplified moment-curvature-based method to analyze the large displacement of the micro-beams. In terms of deformed micro-beam slope, a non-linear differential equation was obtained by using a moment-curvature relation. Numerical results show the static bending of the model has a stiffer behavior than the classical theory.

Arvin [20] investigated free vibration of rotating micro-beams using the strain gradient theory for both Timoshenko and Euler-Bernoulli beam models. The Differential transform method is employed to solve governing differential equations and associated boundary conditions. The results illustrated the natural frequency of vibration is highly sensitive to the rotation speed, length scale parameter, and slenderness ratio. Talimian and Béda [21] studied the dynamic stability analysis of the micro-beams by using the modified couple stress theory. For a simply supported micro-beam with a rectangular cross-section, the effect of geometry on dynamic stability regions is discussed. The outcomes show the material length scale and cross section's height of the micro-beam are effective variables in dynamic stability regions. In another research, Shafiei and Kazemi [22] investigated the buckling of FG micro/nanoporous beams. Using the Euler-Bernoulli beam model, Eringen's nonlocal, and modified couple stress theories governing equations are obtained and solved by the generalized differential quadrature (GDQ) method. For clamped boundary conditions, numerical examples are presented to illustrate the effects of different parameters on the buckling response of the FG porous micro/nanobeams. Moreover, Kamali and Shahabian [23] studied the surface stress effects on buckling and post-buckling behavior of porous nano-plates.

Using the nonlocal strain gradient theory and Euler-Bernoulli beam model, Li et al. [24] performed buckling and vibration analysis of AFG beams. The results showed the AFG beam may exert a softening or hardening effect on the buckling load. Moreover, the natural frequency of vibration is related to size-dependent behavior. In another research, Rezaiee-Pajand and Kamali [25] presented analytical solutions for the post-buckling response of functionally graded micro-beams considering thermal gradients. Including transverse shear deformations, Yang and He [26] studied the buckling and free vibration behavior of AFG micro-beams with the modified couple stress theory. The effects of shear deformation, material gradient index and geometry are depicted in numerical examples. In another work, Sinir et al. [27] presented the non-linear vibration analysis of AFG beams with a non-uniform cross-section considering mid-plane stretching. Frequency-response curves are plotted to depict an unstable zone. Based on the second strain gradient (SSG) theory, a size-dependent formulation for static and dynamic analysis of FG micro/nanobeams was developed by Momeni and Asghari [28]. Numerical examples show a significant difference between SSG theory and other theories for static and free vibration behavior. In another research, Jia et al. [29] studied thermal-mechanical-electrical buckling of FG micro-beams using the Euler-Bernoulli beam model and modified couple stress theory. Including thermal effect, dynamic stability analysis of sandwich FG micro-beams was performed by Al-shujairi and Mollamahmutoglu [30] using nonlocal strain gradient theory. Instability regions are depicted for different boundary conditions. Bhattacharya and Das [31] presented the free vibration behavior of double-tapered, bidirectional FG micro-beams rotating in a thermal environment. Based on the modified couple stress theory, Timoshenko beam model, and Hamilton principle governing equations are obtained.

Unfortunately, unlike a large number of studies available in the field of deterministic analysis, a limited number of researches have addressed the issue of uncertainty in the structural behavior of FGMs. For example, Shegokar and Lal [32] presented the stochastic non-linear static behavior of piezo-electric FG beams subjected to a temperature gradient. A first-order perturbation technique (FOPT) is applied to calculate the mean value and coefficient of variations (COV) of transverse displacement. The effects of various parameters with random material properties on the static response of structure are discussed. Finally, the model is validated with the Monte Carlo simulation (MCS) method. In another work, Xu et al. [33] performed a stochastic dynamic analysis of FGM beams. Random material properties are considered in the model. Free vibration analysis of AFG beams with uncertain material properties was studied by Zhou and Zhang [34]. To model composite material random field, the Karhunen-Loeve expansion is used. For stochastic free vibration analysis, a generalized eigenvalue function is obtained. Then MCS method is applied to compute the statistics of the uncertain model. Indeed, a generalized polynomial chaos expansion is proposed to reduce the computational effort of the MCS method. Recently, Mohammadi et al. [35] presented the pull-in instability of FGM micro-beams with stochastic material properties. The second-order statistics of the pull-in voltage are calculated by both the MCS method and FOPT. Based on the authors' best knowledge, most of the researchers employed random analysis to investigate the mechanical behavior of FGM structures only in macro-scales. The novelty of this research is to study free vibration analysis and estimate the reliability index of a tapered micro-beam made

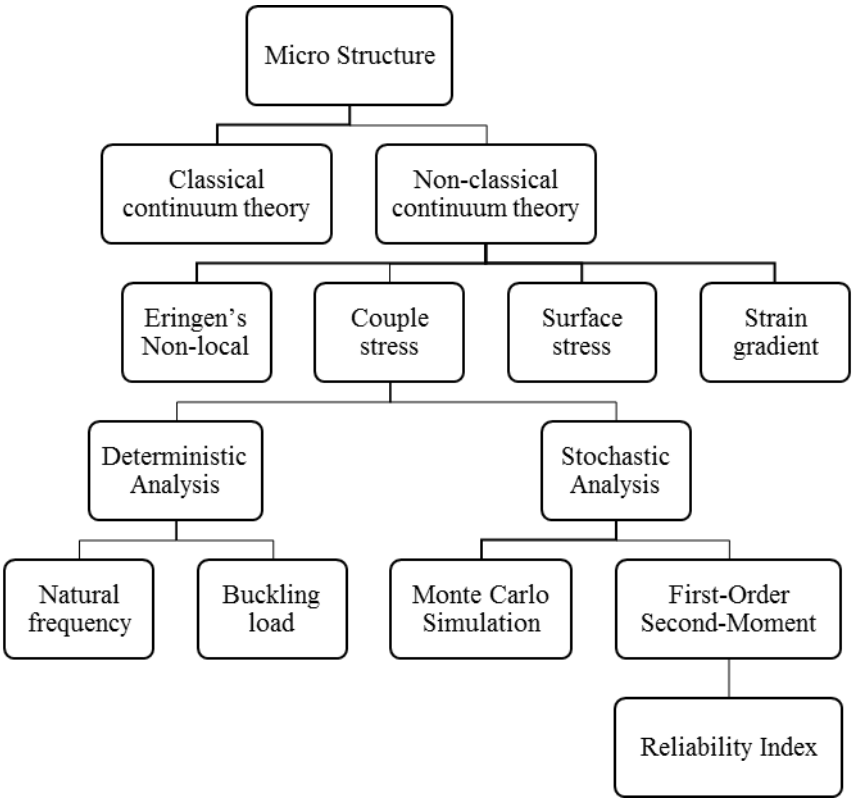

Fig. 1. Flowchart presentation of this work.

from a functionally graded material with random mechanical properties.

Now, the layout of this study is presented. In section 2, mathematical formulations are developed for the free vibration and stability of a tapered AFG micro-beam. The governing equations are obtained by the Hamilton principle and solved using the Galerkin method. Including uncertainties in the mathematical model, the FOSM technique is employed to compute the reliability index of the microstructure. In section 3, some numerical examples are presented to investigate the effects of different parameters on the natural frequency of vibration and the reliability index of the tapered AFG micro-beam. Finally, the main conclusions are presented in section 4. A general view of the paper is presented in the form of a flowchart as illustrated in Fig. 1.

2- Formulation

Based on the modified couple stress theory, the strain energy function for a linear elastic isotropic material can be expressed as:

$$U = \int_V (\sigma_{ij}\varepsilon_{ij} + m_{ij}\chi_{ij})dv \tag{1}$$

In which σ_{ij} and m_{ij} are components of Cauchy stress and couple stress tensors, respectively. Indeed, ε_{ij} and χ_{ij} denote corresponding Green strain and curvature tensors, respectively. They are given by:

$$\sigma_{ij} = \lambda\varepsilon_{nn}\delta_{ij} + 2\mu\varepsilon_{ij} \tag{2a}$$

$$m_{ij} = 2\ell^2\mu\chi_{ij} \tag{2b}$$

$$\varepsilon_{ij} = \frac{1}{2}(u_{i,j} + u_{j,i}) \tag{2c}$$

$$\chi_{ij} = \frac{1}{2}(\theta_{i,j} + \theta_{j,i}) \tag{2d}$$

Where λ and μ are Lame classical constants. Moreover, ℓ is the length scale parameter that models the size-effect behavior. It is a material intrinsic property determined from experiments. $\vec{u}$ stands for displacement field and $\vec{\theta} = \frac{1}{2}Curl(\vec{u})$ is the very small rotation vector.

The initial configuration of an AFG tapered micro-beam

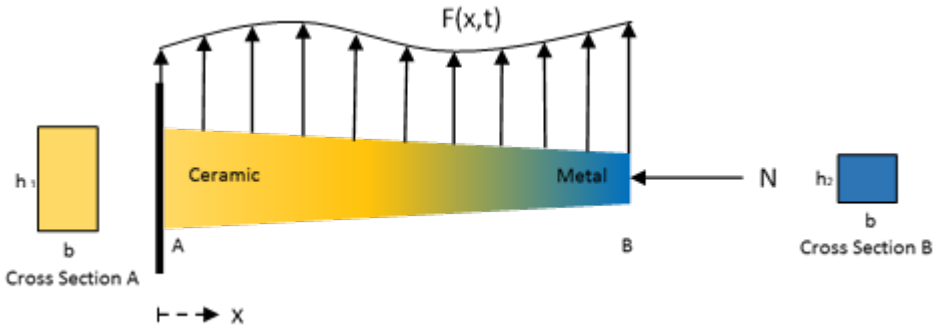

Fig. 2. Initial configuration of AFG tapered micro-beam.

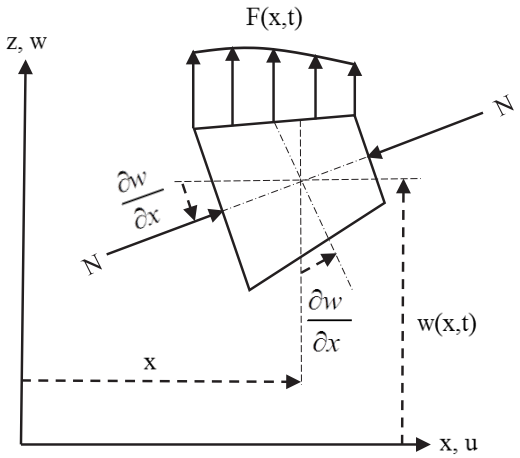

Fig. 3. Deformed shape of the AFG tapered micro-beam.

is shown in Fig. 2. It is subjected to a lateral distributed load F(x,t) and a constant axial force $\overline{N}$ at its free end. The width of the rectangular cross-section has a constant value of b, but its thickness varies linearly from h_1 to h_2 in the entire length of the AFG micro-beam. Mathematically, it can be described as below:

$$h(x) = h_1 + (\frac{h_2 - h_1}{L})x \tag{3}$$

In which h_1 denotes the thickness at clamped support and h_2 is thickness related to the free end. Indeed, L represents the length of the AFG micro-beam.

Using power-law function model, material distribution of FGMs in axial direction of a beam may be expressed as following:

$$\Lambda(x) = \Lambda_c + (\Lambda_m - \Lambda_c)(\frac{x}{L})^n \tag{4}$$

Here, Λ stands for any material property. Subscripts m and c represent metal and ceramic, respectively. Moreover, superscript n called power-law index specifies how materials are distributed along the length of the beam. Here, Young's modulus E, shear modulus μ, and density ρ obey from power distribution rule as follows:

$$\begin{aligned} E(x) &= E_c + (E_m - E_c)(\frac{x}{L})^n \\ \mu(x) &= \mu_c + (\mu_m - \mu_c)(\frac{x}{L})^n \\ \rho(x) &= \rho_c + (\rho_m - \rho_c)(\frac{x}{L})^n \end{aligned} \tag{5}$$

After deformation (See Fig. 3), the components of the displacement field for a beam can be expressed as:

$$\begin{aligned} u_1 &= u(x,t) + z\,\psi(x,t) \\ u_2 &= 0 \\ u_3 &= w(x,t) \end{aligned} \tag{6}$$

Where u represents the axial displacement of the neutral axis of the beam, w is the transverse deflection, and Ψ denotes the rotation angle of the beam cross-section. Given the Euler-Bernoulli beam theory, it is assumed the cross-sections of the beam are perpendicular to the center line and remain plane after deformation. Hence, the angle of rotation can be presented as below:

$$\psi(x,t) \approx -\frac{\partial w(x,t)}{\partial x} \tag{7}$$

The only non-zero strain tensor component can be expressed as:

$$\varepsilon_{11} = \frac{\partial u_1}{\partial x} = \frac{\partial u(x,t)}{\partial x} - z\,\frac{\partial^2 w(x,t)}{\partial x^2} \tag{8}$$

Including the effect of large deflections, the axial strain ε_{11} can be modified by von Kármán nonlinear strain in the following form:

$$\varepsilon_{11} = \frac{\partial u_1}{\partial x} = \frac{\partial u(x,t)}{\partial x} - z\,\frac{\partial^2 w(x,t)}{\partial x^2} + \frac{1}{2}\left(\frac{\partial w(x,t)}{\partial x}\right)^2 \tag{9}$$

The expression $\frac{1}{2}\left(\frac{\partial w(x,t)}{\partial x}\right)^2$ considers the mid-plane stretching. Therefore, the axial component of the Cauchy stress tensor can be expressed as:

$$\sigma_{11} = (\lambda(x) + 2\mu(x))\varepsilon_{11} = \frac{E(x)\nu(x)}{(1+\nu(x))(1-2\nu(x))}\varepsilon_{11} \tag{10}$$

in which ν represents Poisson's ratio. The expression $\frac{\nu(x)}{(1+\nu(x))(1-2\nu(x))}$ called Poisson's effect and can be neglected in beams. Hence, σ_{11} can be rewritten as below:

$$\sigma_{11} = E(x)\left[\frac{\partial u(x,t)}{\partial x} - z\,\frac{\partial^2 w(x,t)}{\partial x^2} + \frac{1}{2}\left(\frac{\partial w(x,t)}{\partial x}\right)^2\right] \tag{11}$$

On the other hand, components of a small rotation vector are given by:

$$\theta_1 = 0 \qquad \theta_2 = -\frac{\partial w(x,t)}{\partial x} \qquad \theta_3 = 0 \tag{12}$$

Therefore, one can calculate the only two non-zero components of curvature tensor and corresponding couple stress tensor fields as below:

$$\chi_{12} = \chi_{21} = -\frac{1}{2}\frac{\partial^2 w(x,t)}{\partial x^2} \tag{13a}$$

$$m_{12} = m_{21} = -\mu(x)\ell^2\,\frac{\partial^2 w(x,t)}{\partial x^2} \tag{13b}$$

The strain energy function of the AFG micro-beam due to bending and mid-plane stretching is given by:

$$U = \frac{1}{2}\int_0^L \int_A \{E(x)[\frac{\partial u(x,t)}{\partial x} - \tag{14}$$

$$z\,\frac{\partial^2 w(x,t)}{\partial x^2} + \frac{1}{2}\left(\frac{\partial w(x,t)}{\partial x}\right)^2]^2 +$$

$$\mu(x)\ell^2[\frac{\partial^2 w(x,t)}{\partial x^2}]^2\}dA\,dx$$

On the other side, the kinetic energy function of the structure can be expressed as below:

$$T = \frac{1}{2}\int_0^L \int_A \{\rho(x)([\frac{\partial u(x,t)}{\partial t} - \tag{15}$$

$$z\,\frac{\partial^2 w(x,t)}{\partial x \partial t}]^2 + [\frac{\partial w(x,t)}{\partial t}]^2)\}dA dx$$

since $\int_A z dA = 0$, one can simplify Eqs. (14) and (15) as:

$$U = \frac{1}{2}\int_0^L \{E(x)A(x)[\frac{\partial u(x,t)}{\partial x} + \frac{1}{2}(\frac{\partial w(x,t)}{\partial x})^2]^2 + (\quad (16a)$$

$$(E(x)I(x) + \mu(x)A(x)\ell^2)[\frac{\partial^2 w(x,t)}{\partial x^2}]^2\}dx$$

$$T = \frac{1}{2}\int_0^L \{\rho(x)A(x)([\frac{\partial u(x,t)}{\partial t}]^2 + \quad (16b)$$

$$[\frac{\partial w(x,t)}{\partial t}]^2) + \rho(x)I(x)[\frac{\partial^2 w(x,t)}{\partial x\,\partial t}]^2\}dx$$

Here, I(x) denotes the second moment of inertia of cross-section at distance x from fixed support, given by $I(x) = \frac{bh(x)^3}{12}$.

The virtual work done by external loads can be expressed as below:

$$\delta W = \int_0^L F(x,t)\delta w dx + \{N\}_{x=0,L} \quad (17)$$

where F(x,t) is the lateral distributed load per unit length and N represents axial force at the ends of the AFG micro-beam. To obtain governing differential equations, Hamilton's principle can be employed in the following form:

$$\int_{t_1}^{t_2} \{\delta T - \delta U + \delta W\}dt = 0 \quad (18)$$

Substituting Eqs. (16a), (16b), and (17) into Eq. (18) lead to the following differential equations and corresponding boundary conditions:

$$\frac{\partial}{\partial x}\{E(x)A(x)[\frac{\partial u(x,t)}{\partial x} + \frac{1}{2}(\frac{\partial w(x,t)}{\partial x})^2]\} = \rho(x)A(x)\frac{\partial^2 u(x,t)}{\partial t^2} \quad (19a)$$

$$\frac{\partial^2}{\partial x^2}\{[E(x)I(x) + \mu(x)A(x)\ell^2]\frac{\partial^2 w(x,t)}{\partial x^2}\} - \frac{\partial}{\partial x}\{\frac{E(x)A(x)}{2}[\frac{\partial w(x,t)}{\partial x}]^3 + [E(x)A(x)\frac{\partial u(x,t)}{\partial x}]\frac{\partial w(x,t)}{\partial x}\} - \frac{\partial}{\partial x}\{\rho(x)I(x)\frac{\partial^3 w(x,t)}{\partial x\,\partial t^2}\} + \rho(x)A(x)\frac{\partial^2 w(x,t)}{\partial t^2} = F(x,t) \quad (19b)$$

$$\{E(x)A(x)[\frac{\partial u(x,t)}{\partial x} + \frac{1}{2}(\frac{\partial w(x,t)}{\partial x})^2] - N\}_{x=0,L} = 0 \quad (19c)$$

or $\{\delta u\}_{x=0,L} = 0$

$$\{\frac{\partial u(x,t)}{\partial t}]\}_{t=t_1,t_2} = 0 \quad \text{or} \quad \{\delta u\}_{t=t_1,t_2} = 0 \quad (19d)$$

$$\{\frac{\partial w(x,t)}{\partial t}]\}_{t=t_1,t_2} = 0 \quad \text{or} \quad \{\delta w\}_{t=t_1,t_2} = 0 \quad (19e)$$

$$\{\frac{\partial^2 w(x,t)}{\partial x\,\partial t}]\}_{t=t_1,t_2} = 0 \quad \text{or} \quad \{\delta(\frac{\partial w(x,t)}{\partial x})\}_{t=t_1,t_2} = 0 \quad (19f)$$

$$\{\rho(x)I(x)\frac{\partial^3 w(x,t)}{\partial x\,\partial t^2} + (E(x)A(x)[\frac{\partial u(x,t)}{\partial x} + \frac{1}{2}(\frac{\partial w(x,t)}{\partial x})^2])\frac{\partial w(x,t)}{\partial x}\} - \frac{\partial}{\partial x}([E(x)I(x) + \mu(x)A(x)\ell^2]\frac{\partial^2 w(x,t)}{\partial x^2})\}_{x=0,L} = 0 \quad (19g)$$

or $\{\delta w\}_{x=0,L} = 0$

$$\{[E(x)I(x) + \mu(x)A(x)\ell^2]\frac{\partial^2 w(x,t)}{\partial x^2}\}_{x=0,L} = 0 \quad (19h)$$

or $\{\delta(\frac{\partial w(x,t)}{\partial x})\}_{x=0,L} = 0$

It is to be noted that axial acceleration $\frac{\partial^2 u(x,t)}{\partial t^2}$ can be neglected. In other words, the right side of Eq. (19a) can be set to zero. Hence, it can be concluded from Eq. (19a) that the expression $E(x)A(x)[\frac{\partial u(x,t)}{\partial x}+\frac{1}{2}(\frac{\partial w(x,t)}{\partial x})^2]$ has a constant value in the entire length of the AFG micro-beam. On the other side, one can rearrange Eq. (19c) as follows:

$$E(x)A(x)[\frac{\partial u(x,t)}{\partial x}+\frac{1}{2}(\frac{\partial w(x,t)}{\partial x})^2]=N \tag{20}$$

Substituting Eq. (20) into Eq. (19b) and performing some manipulations results in:

$$\begin{aligned}&\frac{\partial^2}{\partial x^2}\{[E(x)I(x)+\mu(x)A(x)\ell^2]\frac{\partial^2 w(x,t)}{\partial x^2}\}-\\&N\frac{\partial^2 w(x,t)}{\partial x^2}-\frac{\partial}{\partial x}\{\rho(x)I(x)\frac{\partial^3 w(x,t)}{\partial x\,\partial t^2}\}+\\&\rho(x)A(x)\frac{\partial^2 w(x,t)}{\partial t^2}=F(x,t)\end{aligned} \tag{21}$$

Using Galerkin method, the solution of Eq. (21) can be expressed as:

$$w(x,t)=\varphi(x)q(t) \tag{22}$$

in which φ(x) represents the first mode shape of classic beam and q(t) is function of time t.

Substituting Eq. (22) into Eq. (21) leads to the following:

$$\begin{aligned}&[\rho(x)A(x)\varphi(x)-\\&\frac{d}{dx}\{\rho(x)I(x)\frac{d\varphi(x)}{dx}\}]\frac{d^2 q(t)}{dt^2}+\\&[\frac{d^2}{dx^2}\{(E(x)I(x)+\\&\mu(x)A(x)\ell^2)\frac{d^2\varphi(x)}{dx^2}\}-\\&N\frac{d^2\varphi(x)}{dx^2}]\frac{dq(t)}{dt}=F(x,t)\end{aligned} \tag{23}$$

Integrating Eq. (23) with respect to x from x = 0 to x = L results in below expression:

$$H_1\frac{d^2 q(t)}{dt^2}+H_2\frac{dq(t)}{dt}=\int_0^L F(x,t)dx \tag{24}$$

where

$$H_1=\int_0^L[\rho(x)A(x)\varphi(x)- \tag{25a}$$

$$\frac{d}{dx}\{\rho(x)I(x)\frac{d\varphi(x)}{dx}\}]dx$$

$$H_2=\int_0^L[\frac{d^2}{dx^2}\{(E(x)I(x)+ \tag{25b}$$

$$\mu(x)A(x)\ell^2)\frac{d^2\varphi(x)}{dx^2}\}-N\frac{d^2\varphi(x)}{dx^2}]dx$$

Expressions H_1 and H_2 represent the equivalent mass and stiffness of the AFG micro-beam, respectively. It should be noted that φ(x) (the first mode shape) for a cantilevered beam is given by Rao [36]:

$$\begin{aligned}\varphi(x)=&\sin(1.88\frac{x}{L})-\sinh(1.88\frac{x}{L})+\\&1.36\cosh(1.88\frac{x}{L})-1.36\cos(1.88\frac{x}{L})\end{aligned} \tag{26}$$

For free vibration analysis, the right side of Eq. (24) must be set to zero. The natural frequency of vibration for the AFG tapered micro-beam can be obtained as:

$$\omega_n=\sqrt{\frac{H_2}{H_1}} \tag{27}$$

Given Eq. (25b), it is obvious that by increasing the axial force N, the stiffness of the system will reduce. Therefore, a critical value of N indicating instability condition of the structure can be obtained by setting H_2 to zero as follows:

$$N_{cr}=\frac{\int_0^L[\frac{d^2}{dx^2}\{(E(x)I(x)+\mu(x)A(x)\ell^2)\frac{d^2\varphi(x)}{dx^2}\}]dx}{\int_0^L[\frac{d^2\varphi(x)}{dx^2}]dx} \tag{28}$$

Table 1. Mechanical properties of the AFG micro-beam.

	Metal	Ceramic
Modulus of elasticity (*E*)	100 GPa	220 GPa
Material density (*ρ*)	7850 kg/m^3	6100 kg/m^3
Poisson ratio (*v*)	0.3	0.3

For stochastic analysis, consider a limit state function defined as g = R-Q in which R and Q represent load-carrying capacity (resistance) and load effect (demand), respectively. As a measure of structural safety, when g > 0, the resistance is greater than demand and the structure will remain safe and vice versa. The reliability index can be calculated as [14]:

$$\beta = \frac{\Gamma_R - \Gamma_Q}{\sqrt{S_R^2 + S_Q^2}} \tag{29}$$

Using Taylor series expansion, a linearized approximation for a non-linear limit state function of random variables g can be presented as below:

$$g(X_1, X_2, ..., X_n) \approx g(x_1^*, x_2^*, ..., x_n^*) + \tag{30}$$

$$\sum_{i=1}^{n} (X_i - x_i^*) \frac{\partial g}{\partial X_i}\bigg|_{evaluated\ -at\ (x_1^*, x_2^*, ..., x_n^*)}$$

It should be noted that (x_1^*, x_2^*... x_n^*) is the point at which the expansion is performed. One choice for this point can be selected as the corresponding expected values of random variables. Therefore, the Eq. (30) becomes:

$$g(X_1, X_2, ..., X_n) \approx g(\Gamma_{X_1}, \Gamma_{X_2}, ..., \Gamma_{X_n}) + \tag{31}$$

$$\sum_{i=1}^{n} (X_i - \Gamma_{X_i}) \frac{\partial g}{\partial X_i}\bigg|_{evaluated\ -at\ -\text{expected}\ -values}$$

Based on the definition of the reliability index introduced by Hasofer and Lind (1974), it is the inverse of the coefficient of variation of the limit state function g [17]. According to the first-order second-moment method, the relation for computing the reliability index can be expressed as below:

$$\beta = \frac{g(\Gamma_{X_1}, \Gamma_{X_2}, ..., \Gamma_{X_n})}{\sqrt{\sum_{i=1}^{n} (a_i S_{X_i})^2}} \tag{32}$$

in which β is the reliability index. Moreover, Γ_X and S_X stand for expected value and standard deviation of random variables, respectively. Furthermore, $a_i = \frac{\partial g}{\partial X_i}\Big|_{at\ -x_i^* = \Gamma_{x_i}}$ is the partial derivative of limit state function concerning each random variable evaluated at expected values. It is called first-order due to employing first-order terms in Taylor series expansion and the second moment due to using means and variances, only. It should be noted that the probability of failure can be computed as $P_f = \Phi(-\beta)$, where Φ is the value of the cumulative distribution function (CDF) of a random variable with a standard normal probability distribution.

As discussed before, a linear approximation for the natural frequency of vibration ω_n obtained from Eq. (27) can be written as:

$$\omega_n(X) = \omega_n(\Gamma_X) + (X - \Gamma_X) \frac{\partial \omega_n}{\partial X}\bigg|_{X=\Gamma_X} \tag{33}$$

in which X can stand for any random variable.

3- Numerical Examples

In this section, some numerical examples are presented to illustrate the free vibration response and stability of a tapered AFG micro-beam subjected to a constant axial load. The mechanical properties of the microstructure are listed in Table 1. First, the deterministic analysis of free vibration and

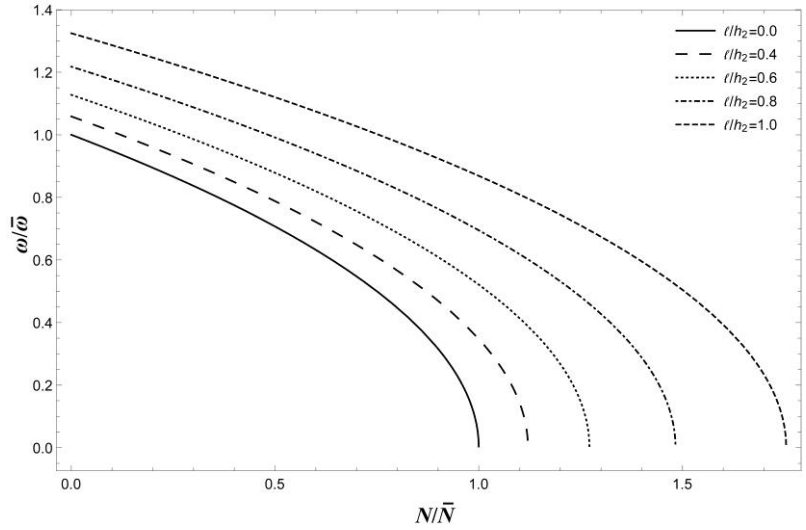

Fig. 4. The natural frequency of vibration of the AFG micro-beam versus axial load with L=100µm, b=10µm, h1=2h2=10µm, and n=2.

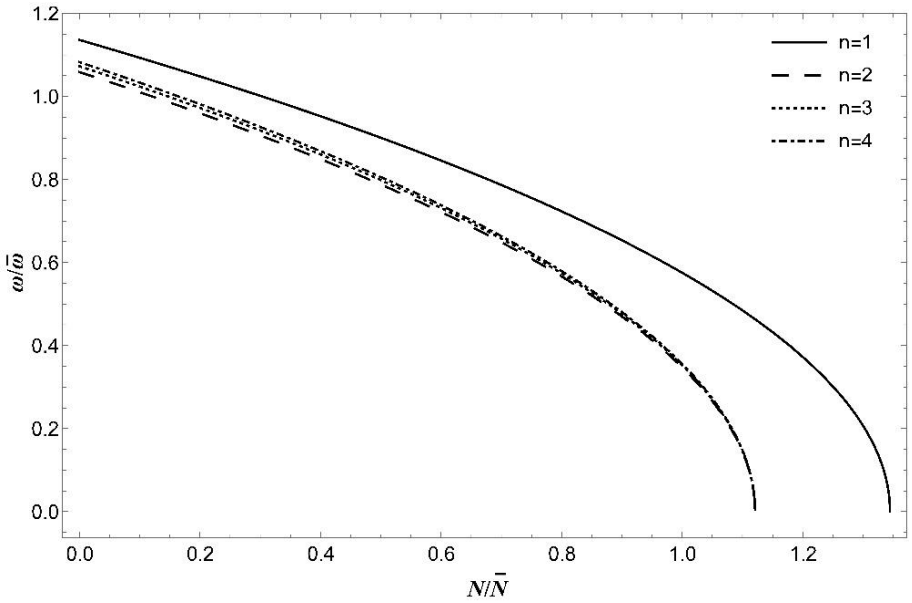

Fig. 5. The natural frequency of vibration of the AFG micro-beam versus axial load with L=100µm, b=10µm, h1=2h2=10µm, and ℓ=2µm.

stability is studied. Then, the reliability index of the micro-structure is investigated considering uncertainty in material properties.

3- 1- Deterministic analysis

For the case L = 100µm, b = 10µm, $h_1 = 2h_2 = 10$µm, and n = 2 variation of the natural frequency of vibration via the axial load is plotted in Fig. 4 for different values of the length scale parameter. The vertical axis is normalized with the linear classic natural frequency of vibration $\overline{\omega} = 1.03 \times 10^7$ rad/sec, which is computed by vanishing the length scale parameter and the axial load from Eq. (27). The horizontal axis is normalized with the classic critical axial load $\overline{N} = 135786$ µN calculated by setting the length scale parameter to zero in Eq. (28). It can be observed that by increasing axial load, the natural frequency of vibration reduces until it reaches zero. Moreover, size-dependent behavior has a significant influence on the free vibration response of the AFG tapered micro-beam. The more value of the length scale parameter, the more natural frequency of vibration.

Effect of the material property distribution is depicted in Fig. 5 for the case L = 100µm, b = 10µm, $h_1 = 2h_2 = 10$µm, and $\ell = 2$µm. Variation of the normalized natural frequency of vibration is plotted versus the normalized axial load for

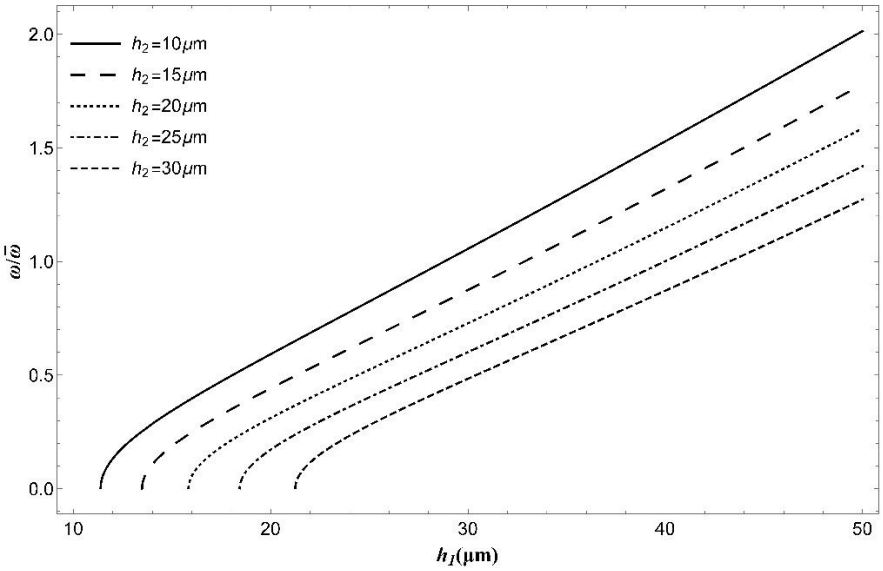

Fig. 6. The natural frequency of vibration of the AFG micro-beam versus thickness with L=300μm, b=10μm, ℓ=8μm, n=2, and N = 40000μN.

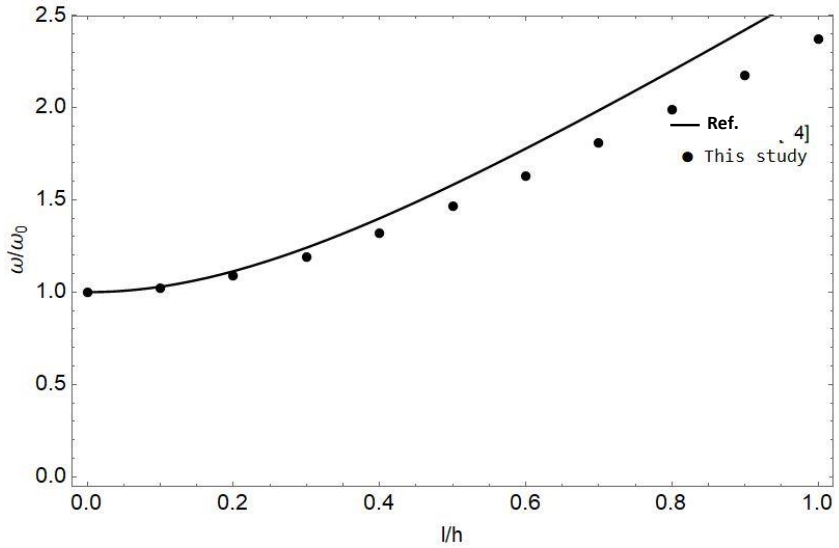

Fig. 7. The dimensionless natural frequency of vibration of the simple prismatic micro beam without axial load.

different values of the power-law index. It can be seen that the nonlinear distribution of material properties in the axial direction reduces the natural frequency of vibration. The variation of the power-law index in the nonlinear regime has no considerable influence on the free vibration behavior of the AFG micro-beam.

Finally, the effect of the non-uniform cross-section is investigated. Variation of the normalized natural frequency of vibration versus different geometries of the micro-structure is plotted in Fig. 6. It should be noted that $\omega_{CL} = 4.15\times10^6$ rad/sec is computed for the case L = 300μm, b = 10μm, h_1 = $3h_2$ = 30μm, n = 2, and N = 40000μN. As can be seen, when thickness at the free end h_2 is constant, increasing thickness at fixed support h_1 results in a higher natural frequency of vibration. On the other side, by enhancing the thickness at the free end h_2 while the thickness at the fixed support is constant, the natural frequency of vibration will reduce. It can be concluded when the thickness at fixed support is bigger than the thickness at the free end, more stability is expected.

3- 2- On verification of the results

In this section, for a simpler case, the results are numerically validated with known data in the literature [37]. For this purpose, it is assumed that the prismatic micro-beam is made from only one constituent material without axial load at its free end. The variation of the natural frequency of vibration versus the length scale parameter is illustrated in Fig. 7. Good accuracy is observed by comparing numerical

Table 2. Probability of failure for different reliability indices.

β	P_f
1	1.59×10^{-1}
2	2.28×10^{-2}
3	1.35×10^{-3}
4	3.17×10^{-5}
5	2.87×10^{-7}
6	9.87×10^{-10}
7	1.28×10^{-12}
8	6.22×10^{-16}

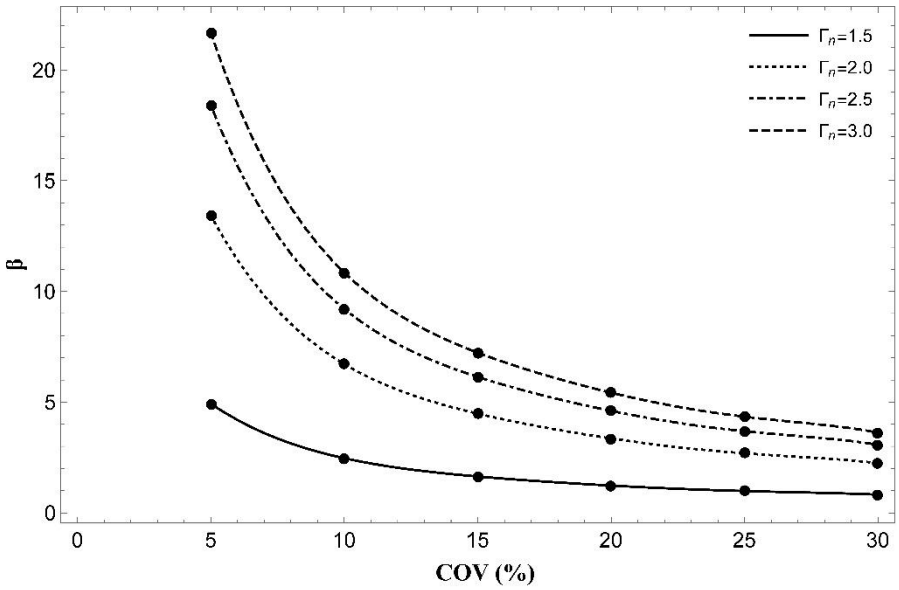

Fig. 8. Reliability index of the AFG micro-beam with L=100μm, b=10μm, h1=2h2=10μm, ℓ=2μm, and N=152170μN.

results between analytical solutions presented in this paper with data reported in the literature [37]. It should be noted that ω_0 is obtained by omitting the size-dependent behavior (ℓ=0).

3- 3- Reliability analysis

Here, reliability analysis of the AFG tapered micro-beam is considered. Failure can be defined as vanishing the effective stiffness of the microstructure due to the influence of the compressive axial force acting on the free end of the microstructure. The reliability index can be computed from the FOSM method as mentioned in Eq. (32). The Probability of failure P_f for some values of the reliability index β is presented in Table 2. As mentioned before, there are some uncertainties due to the fabrication process of FG micro-beams.

At first, it is assumed that the material distribution gradient is a random variable. The reliability index of the micro-structure via different COVs (5, 10, 15, 20, 25, and %30) and the expected value of the power-law index (1.5, 2, 2.5, and 3) are plotted in Fig. 7. It can be observed that by enhancing the mean value of the power-law index of samples, the reliability index of the AFG micro-beam increases. In other words, the probability of failure will decrease. When the expected value of the material index enhances from 1.5 to 3, the reliability index of the micro-structure becomes 4.4 times greater. On the other side, enhancing the COV of the samples leads to increasing the probability of failure until it approaches a constant value.

The variation of the reliability index versus different mean values (1, 1.5, 2, and 2.5μm) and COVs (5, 10, 15, 20, 25, and %30) of the length scale parameter is shown in Fig. 8. It can be seen that by enhancing the size-dependent effect, the reliability of the micro-structure will increase. It is interesting

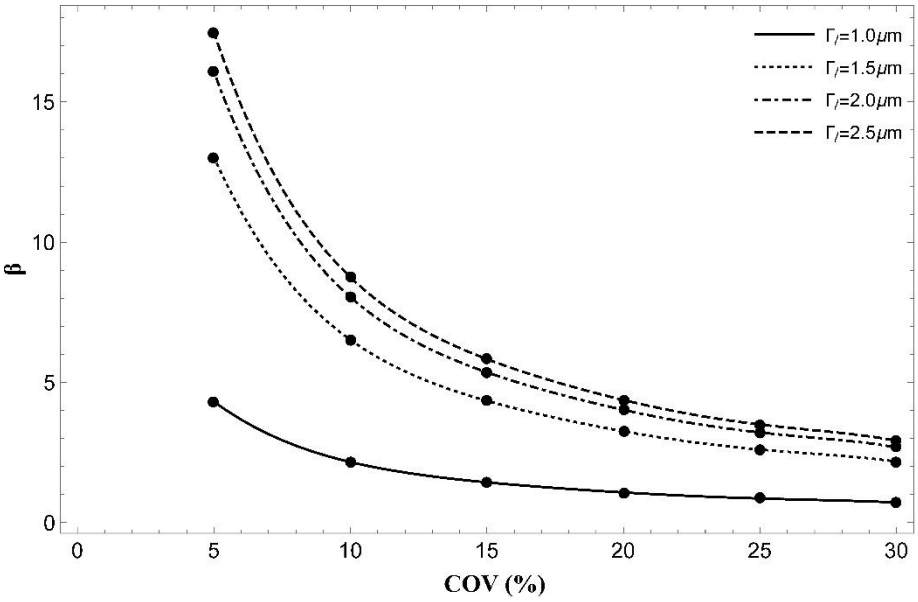

Fig. 9. Reliability index of the AFG micro-beam with L=100μm, b=10μm, h1=2h2=10μm, n=2, and N=139000μN.

to note that the reliability index β of samples with $\Gamma_\ell = 2.5$ μm is about four times more than samples with $\Gamma_\ell = 1$ μm. On the other hand, whatever samples have more deviations from their mean values, more probability of failure is expected.

Finally, it is assumed that the axial load is not a deterministic parameter. Variation of reliability index via various COVs (5, 10, 15, 20, 25, and %30) and expected value of the axial load (125×10^3, 130×10^3, 135×10^3, and 140×10^3μN) is plotted in Fig. 9. It is obvious that by reducing the compressive axial force, the reliability of the AFG tapered micro-beam increases. For example, if the mean value of the compressive axial load reduces from 10×140^3 to 125×10^3μN, the reliability index becomes 2.5 times higher. Again, for all samples with high COV, the probability of failure approaches a constant value.

4- Conclusion

In this study, free vibration and stability of a cantilevered axially functionally graded micro-beam with a non-uniform cross-section and random material properties are investigated. Numerical examples for both deterministic and reliability analysis are presented to show the effects of different parameters on the natural frequency of vibration and stability of the microstructure. The following results can be obtained:

Due to the effect of nonlinear geometry, the natural frequency of vibration is dependent on the axial force. Enhancing the compressive axial force results in decreasing the effective stiffness of the AFG tapered micro-beam. For a critical value of the axial load N_{cr}, the system becomes unstable.

By enhancing the length scale parameter, a higher natural frequency of vibration is expected. In other words, size-dependent behavior enhances the effective stiffness of the AFG tapered micro-beam.

In comparison with the non-linear distribution of material properties (n > 1), a linear distribution (n = 1) leads to a higher natural frequency of vibration. However, there is no significant difference in the free vibration behavior of the AFG micro-beam when the power-law index varies in the non-linear regime.

The non-uniform cross-section has a remarkable influence on the stability of the cantilevered AFG micro-beam. When the thickness of the cross-section at the free end h_2 increases and the thickness of the cross-section at the fixed support h_1 decreases, the stability of the microstructure will reduce.

By increasing the coefficient of variation (COV) of random variables, the reliability index will decrease. Indeed, the probability of failure approaches a constant value.

For a constant coefficient of variation, more non-linear material distribution and higher length scale parameters increase the reliability of the AFG micro-beam.

Data Availability Statement: All data, models, and code generated or used during the study appear in the submitted article.

Funding: This research did not receive any specific grant from funding agencies in the public, commercial, or not-for-profit sectors.

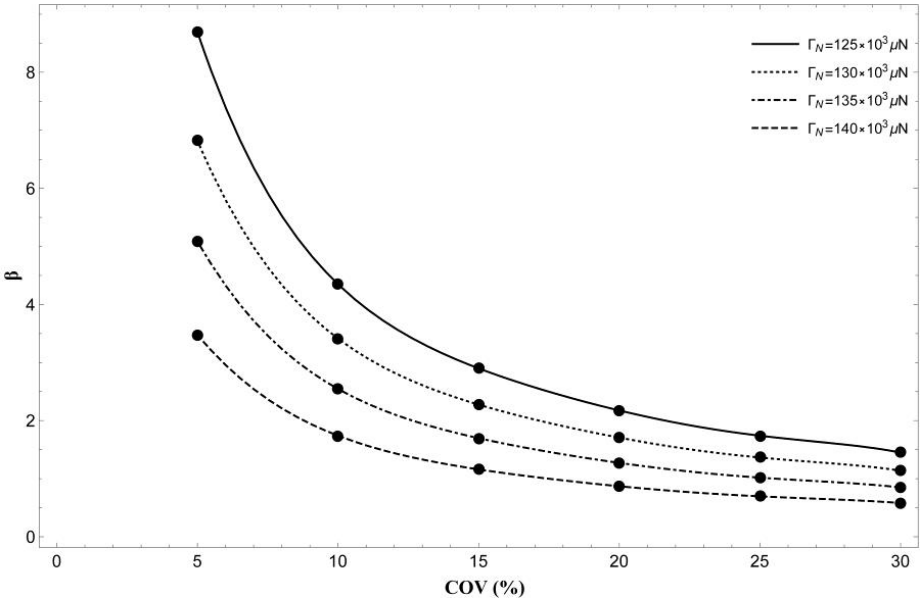

Fig. 10. Reliability index of the AFG micro-beam with L=100μm, b=10μm, h1=2h2=10μm, ℓ=2μm, and n=2.

References

[1] Michael, CY. Kwok, Piezoelectric micro-lens actuator, Sensors and Actuators A: Physical, 236 (2015) 116-129.

[2] R. Fan, Y. Luo, L. Li, Q. Wu, Z. Ren, B. Peng, Large-range fiber microsphere micro-displacement sensor, Optical Fiber Technology, 48 (2019) 173-178.

[3] W. Ma, T. Huang, S. Guo, C. Yang, Y. Ding, C. Hu, Atomic force microscope study of the aging/rejuvenating effect on asphalt morphology and adhesion performance, Construction and Building Materials, 205 (2019) 642-655.

[4] M. Li, Y. Liu, L. Dong, C. Shen, F. Li, M. Huang, C. Ma, B. Yang, X. An, W. Sand, Recent advances on photocatalytic fuel cell for environmental applications-The marriage of photocatalysis and fuel cells, Science of the Total Environment, 668 (2019) 966-978.

[5] J. Ding, Y. Tian, L.S. Wang, X. Huang, H.R. Zheng, K. Song, X.G. Zeng, Micro-mechanism of the effect of grain size and temperature on the mechanical properties of polycrystalline TiAl, Computational Materials Science, 158 (2019) 76-87.

[6] J. Kabel, Y. Yang, M. Balooch, C. Howard, T. Koyanagi, K.A. Terrani, Y. Katoh, P. Hosemann, Micro-mechanical evaluation of SiC-SiC composite interphase properties and debond mechanisms, Composites Part B: Engineering, 131 (2017) 173-183.

[7] A.C. Eringen, Linear theory of micropolar elasticity, Mathematics and Mechanics of Solids, 15 (6) (1966) 909-923.

[8] R.D. Mindlin, N.N. Eshel, On first strain-gradient theories in linear elasticity, International Journal of Solids and Structures, 4 (1) (1968) 109-124.

[9] E. Cosserat, F. Cosserat, Théorie des corps déformables, (1909).

[10] W.T. Koiter, Couple-stress in the theory of elasticity, Proc K Ned Akad Wet C, 67 (1964) 17-44.

[11] R.D. Mindlin, Second gradient of strain and surface-tension in linear elasticity, International Journal of Solids and Structures, 1 (4) (1965) 417-438.

[12] R.A. Toupin, Elastic materials with couple-stresses, Archive for Rational Mechanics and Analysis, 11 (1) (1962) 385-414.

[13] J. Qiu, J. Tani, T. Ueno, T. Morita, H. Takahashi, H. Du, Fabrication and high durability of functionally graded piezoelectric bending actuators, Smart Materials and Structures, 12 (1) (2003) 115-121.

[14] Y. Xu, Y. Qian, J. Chen, G. Song, Stochastic dynamic characteristics of FGM beams with random material properties, Composite Structures, 133 (2015) 585-594.

[15] F. Ferrante, L. Graham-Brady, Stochastic simulation of non-Gaussian/nonstationary properties in a functionally graded plate, Computer Methods in Applied Mechanics and Engineering, 194(12) (2005) 1675-1692.

[16] S. Kitipornchai, J. Yang, K. Liew, Random vibration of the functionally graded laminates in thermal environments, Computer Methods in Applied Mechanics and Engineering, 195(9) (2006) 1075-1095.

[17] A.S. Nowak, K.R. Collins, Reliability of structures, CRC Press (2012).

[18] Wang, J. Zhao, S. Zhou, A micro scale Timoshenko

beam model based on strain gradient elasticity theory, European Journal of Mechanics - A/Solids, 29 (4) (2010) 591–599.

[19] B.N. Patel, D. Pandit, S.M. Srinivasan, A simplified moment-curvature based approach for large deflection analysis of micro-beams using the consistent couple stress theory, European Journal of Mechanics - A/Solids, 66 (2017) 45–54.

[20] H. Arvin, Free vibration analysis of micro rotating beams based on the strain gradient theory using the differential transform method: Timoshenko versus Euler-Bernoulli beam models, European Journal of Mechanics - A/Solids, 65 (2017) 336–348.

[21] A. Talimian, P. Béda, Dynamic stability of a size-dependent micro-beam, European Journal of Mechanics - A/Solids, 72 (2018) 245-251.

[22] N. Shafiei, M. Kazemi, Nonlinear buckling of functionally graded nano-/micro-scaled porous beams, Composite Structures, 178 (2017) 483-492.

[23] F. Kamali, F. Shahabian, Analytical solutions for surface stress effects on buckling and post-buckling behavior of thin symmetric porous nano-plates resting on elastic foundation, Archive of applied mechanics, 91 (2021) 2853-2880.

[24] X. Li, L. Li, Y. Hu, Z. Ding, W. Deng, Bending, buckling and vibration of axially functionally graded beams based on nonlocal strain gradient theory, Composite Structures, 165 (2017) 250-265.

[25] M. Rezaiee-Pajand, F. Kamali, Exact solution for thermal-mechanical post-buckling of functionally graded micro-beams, CEAS Aeronautical Journal, 12 (2021) 85-100.

[26] W. Yang, D. He, Free vibration and buckling analyses of a size-dependent axially functionally graded beam incorporating transverse shear deformation, Results in Physics, 7 (2017) 3251-3263.

[27] S. Sınır, M. Çevik, B.G. Sınır, Nonlinear free and forced vibration analyses of axially functionally graded Euler-Bernoulli beams with non-uniform cross-section, Composites Part B: Engineering, 148 (2018) 123-131.

[28] S.A. Momeni, M. Asghari, The second strain gradient functionally graded beam formulation, Composite Structures, 188 (2018) 15-24.

[29] X.L. Jia, L.L. Ke, X.L. Zhong, Y. Sun, J. Yang, S. Kitipornchai, Thermal-mechanical-electrical buckling behavior of functionally graded micro-beams based on modified couple stress theory, Composite Structures, 202 (2018) 625-634.

[30] M. Al-shujairi, Dynamic stability of sandwich functionally graded micro-beam based on the nonlocal strain gradient theory with thermal effect, Composite Structures, 201 (2018) 1018-1030.

[31] S. Bhattacharya, D. Das, Free vibration analysis of bidirectional-functionally graded and double-tapered rotating micro-beam in thermal environment using modified couple stress theory, Composite Structures, 215 (2019) 471-492.

[32] N.L. Shegokar, A. Lal, Stochastic nonlinear bending response of piezoelectric functionally graded beam subjected to thermoelectromechanical loadings with random material properties, Composite Structures, 100 (2013) 17-33.

[33] Y. Xu, Y. Qian, J. Chen, G. Song, Stochastic dynamic characteristics of FGM beams with random material properties, Composite Structures, 133 (2015) 585-594.

[34] Y. Zhou, X. Zhang, Natural frequency analysis of functionally graded material beams with axially varying stochastic properties, Applied Mathematical Modelling, 67 (2019) 85-100.

[35] M. Mohammadi, M. Eghtesad, H. Mohammadi, Stochastic analysis of pull-in instability of geometrically nonlinear size-dependent FGM micro beams with random material properties, Composite Structures, 200 (2018) 466-479.

[36] S.S. Rao, Vibration of continuous systems, New York: Wiley, (2007)

[37] S. Kong, S. Zhou, Z. Nie, K. Wang, The size-dependent natural frequency of Bernoulli-Euler micro-beams, International Journal of Engineering Science, 46 (2008) 427-437.

HOW TO CITE THIS ARTICLE

F. Kamali, F. Shahabian, Free Vibration of Axially Functionally Graded Tapered Micro-Beams Considering Uncertain Properties, AUT J. Civil Eng., 5(4) (2021) 543-556.

DOI: 10.22060/ajce.2022.18056.5657